Acta Pharmaceutica Sinica B 2026;16(3):1747−1761

Chinese Pharmaceutical Association
Institute of Materia Medica, Chinese Academy of Medical Sciences

Acta Pharmaceutica Sinica B

www.elsevier.com/locate/apsb
www.sciencedirect.com

ORIGINAL ARTICLE

bHLH130 mediates gibberellin signaling to regulate tanshinone biosynthesis in *Salvia miltiorrhiza*

Haizheng Yu[a,†], Ruiyang Yao[a,†], Sixue Zhang[b], Yongxing Chen[a], Caiyan Liang[b], Yijing Liu[b], Wenrui Li[d], Bingcong Xing[c,*], Dongfeng Yang[b,*], Lei Zhang[a,b,*]

[a]*Department of Pharmaceutical Botany, School of Pharmacy, Naval Medical University, Shanghai 200433, China*
[b]*Innovative Drug Research Center, Zhejiang Province Key Laboratory of Plant Secondary Metabolism and Regulation, College of Life Sciences and Medicine, Zhejiang Sci-Tech University, Hangzhou 310018, China*
[c]*Zhejiang Provincial Key Laboratory of Resources Protection and Innovation of Traditional Chinese Medicine, Zhejiang A&F University, Hangzhou 311300, China*
[d]*School of Food Science and Engineering, Shaanxi University of Science and Technology, Xi'an 710021, China*

Received 26 March 2025; received in revised form 6 August 2025; accepted 21 October 2025

KEY WORDS

Salvia miltiorrhiza;
Tanshinone;
bHLH;
DELLA;
Secondary metabolic regulation;
Gibberellic acid;
Transcription factor;
Transcriptional regulation

Abstract *Salvia miltiorrhiza* is a prominent traditional Chinese medicinal (TCM) herb with notable therapeutic applications, especially in treatment of cardiovascular and cerebrovascular diseases. A crucial role in promoting tanshinone biosynthesis is attributed to the gibberellic acid (GA) signaling pathway; however, its precise regulatory mechanisms remain incompletely understood. In the current investigation, we identified bHLH130, a GA-responsive bHLH transcription factor (TF), *via* transcriptomic analysis of GA-treated hairy roots from *S. miltiorrhiza*. Functional analysis demonstrated that *bHLH130* overexpression markedly suppressed tanshinone biosynthesis, whereas its knockout resulted in elevated tanshinone accumulation. Additionally, it was confirmed that bHLH130 directly targets E-box motifs within the promoters of biosynthetic genes, including *DXS2*, *CPS1*, *KSL1*, and *CYP76AH1*, thereby negatively regulating their transcriptional activities. Moreover, bHLH130 interacts with DELLA4, forming a regulatory complex implicated in the modulation of tanshinone biosynthesis. Co-overexpression assays revealed that *DELLA4* attenuated the inhibitory effects of *bHLH130* on tanshinone accumulation. Collectively, our data propose that the bHLH130−DELLA4 interaction constitutes a critical regulatory node, balancing GA signaling with secondary metabolite production and offering novel strategies for the

*Corresponding authors.
E-mail addresses: idrc@zstu.edu.cn (Lei Zhang), ydf807@sina.com (Dongfeng Yang), xingbingcong@163.com (Bingcong Xing).
†These authors made equal contributions to this work.

Peer review under the responsibility of Chinese Pharmaceutical Association and Institute of Materia Medica, Chinese Academy of Medical Sciences.

https://doi.org/10.1016/j.apsb.2025.11.041

metabolic engineering of tanshinones. In conclusion, this research delineates the regulatory role of bHLH130 in tanshinone synthesis, providing valuable insights into the GA-mediated modulation of secondary metabolism.

1. Introduction

Plants produce a diverse array of secondary or specialized metabolites *via* species-specific metabolic pathways. These pathways are driven by core metabolic processes and collectively form a complex network. Specialized metabolites play essential roles in growth, cellular replenishment, whole-plant resource allocation, and adaptation to environmental changes[1]. Furthermore, these metabolites significantly benefit human health and survival. Throughout history, bioactive metabolite derived from plants have been consistently employed in the treatment of various diseases, forming the cornerstone of modern drug discovery and development. Over 30% of current drugs are directly derived from plants, and more than 60% of drugs approved in the past two decades originate from plant extracts or their derivatives[1,2].

Medicinal herbs represent a valuable reservoir of natural compounds widely utilized in diverse traditional medicinal systems[3,4]. According to the fourth national survey of Chinese medicinal resources, there are 15,227 identified medicinal plants in China, which serve as the cornerstone of the brilliant culture of TCM[3,5]. Among these, *Salvia miltiorrhiza* is a renowned plant indigenous to Eastern Asia. Its desiccated roots and rhizomes, commonly termed "Danshen" in TCM, were initially recorded in *The Divine Farmer's Materia Medica* (approximately A.D. 102−200)[6]. Currently, Danshen remains extensively applied in clinical practice for preventing and treating ailments such as hypertension, coronary heart disease, and atherosclerosis[7]. Tanshinones, the representative diterpenoid secondary metabolites of *S. miltiorrhiza*, exhibit profound pharmacological effects[8], as supported by contemporary research demonstrating their efficacy in promoting blood circulation and alleviating blood stasis, dysmenorrhea, and amenorrhea[9]. Given their distinct structural characteristics and substantial medicinal value, considerable advancements have been achieved in elucidating their biosynthetic processes.

The biosynthetic pathway of tanshinones consists of three primary stages: the initial generation of geranylgeranyl pyrophosphate (GGPP), subsequent cyclization into hypotanshinone dienes, and final structural modifications. The synthesis of GGPP, the first phase, resembles the biosynthetic pathways observed in other diterpenoids, originating from either the 2-*C*-methyl-D-erythritol 4-phosphate (MEP) or mevalonate (MVA) pathways. Rate-limiting enzymes in these pathways, including DXS and DXR from the MEP pathway and HMGS and HMGR from the MVA pathway, substantially influence tanshinone biosynthesis[10]. The subsequent cyclization of GGPP into hypotanshinone dienes involves enzymatic catalysis by terpene synthases/cyclases (TPSs), notably copalyl diphosphate synthase (CPS) and kaurene synthase-like (KSL). The final stage consists of diverse tanshinone formation through various cytochrome P450 enzymes, including SmCYP76AH1, SmCYP76AH3, SmCYP76AK1, SmCYP76AK2, SmCYP76AK3, SmCYP71D373, and SmCYP71D375[11-14]. To date, most key enzyme genes involved in tanshinone biosynthesis have been cloned and functionally characterized.

However, like many plant-derived bioactive compounds beneficial to human health, tanshinones naturally accumulate only in trace amounts in plants. Their complex chemical structures complicate industrial-scale synthesis, making supplies vulnerable to shortages and impacting security of the clinical therapeutics. Therefore, establishing efficient and stable methodologies to enhance tanshinone yield is imperative. The production of specialized metabolites is controlled through an elaborate regulatory network operating at various biological layers, including mechanisms mediated by transcription, post-transcription, translation, post-translation, and chromatin remodeling[15]. Transcriptional regulation, the initial step from genome to proteome, critically determines the final accumulation of secondary metabolites[15]. Consequently, TFs serve as powerful tools to manipulate plant secondary metabolism[16].

Over 1300 transcription factors (TFs) belonging to various families, such as MYB, WRKY, bHLH, and WD40, have been discovered in *S. miltiorrhiza*[17]. Notably, MeJA induces SmMYB97, enabling it to bind *cis*-regulatory elements within *SmCPS1* and *SmKSL1* promoter regions. Such binding modulates their transcriptional activity, subsequently promoting the biosynthesis of tanshinones[18]. Additionally, MYC2 directly activates the *SmGGPPS1* promoter and engages in protein−protein interactions with SmMYB36, enhancing SmMYC2-mediated transcriptional activation of *SmGGPPS1*, further stimulating tanshinone accumulation[19]. In addition, SmMYB36 serves as an activator of *SmERF6* and *SmERF115* transcription, indirectly promoting the synthesis of tanshinones and phenolic acids within *S. miltiorrhiza* hairy root cultures[20]. Prior investigations have revealed that SmbHLH10 also acts as a positive transcriptional modulator of tanshinone production in hairy roots[21]. Similarly, overexpression of *SmWD40-2* stimulates the expression of most genes involved in the tanshinone biosynthetic pathway, underscoring its utility in metabolic engineering applications for *S. miltiorrhiza*[17].

The biosynthesis and accumulation of bioactive constituents in medicinal herbs are tightly regulated by complex transcriptional networks associated with hormone signaling pathways. Gibberellic acid (GA), a critical plant hormone, governs diverse physiological processes, including developmental progression, responses to stress, and secondary metabolite biosynthesis[22]. In recent years, significant advances have elucidated the various components involved in GA signaling, among which DELLA proteins function as primary repressors, playing critical roles in the plant's response to GA stimuli. In *Arabidopsis thaliana*, five DELLA proteins (GAI, RGA, RGL1, RGL2, and RGL3) have been identified. In contrast, rice has only one DELLA protein (SLR1)[23], while maize possesses two DELLA proteins (DWARF8 (D8) and D9)[24]. In addition, four DELLA proteins (DELLA1−4) have been found in *S. miltiorrhiza*[25]. GA-INSENSITIVE DWARF 1 (GID1) functions as the receptor for GA. Upon GA binding, GID1 undergoes a conformational change and interacts with DELLA proteins. The

$SCF^{SLY1/GID2}$ ubiquitin E3 ligase complex is recruited by this interaction, prompting the ubiquitination and subsequent proteolysis of DELLA proteins through the 26S proteasome. The degradation of DELLA proteins liberates transcription factors, which in turn induce GA-responsive genes, initiating essential physiological events such as seed germination, leaf enlargement, flowering, stem growth, and secondary metabolite production[26-28]. Despite notable advancements, the specific influence of GA on secondary metabolic pathways in *S. miltiorrhiza* has yet to be fully elucidated.

Our previous research established that exogenous application of GA enhances tanshinone production in *S. miltiorrhiza* hairy roots[29]. Despite identification of pivotal GA signaling-related TFs, such as SmGRAS1, SmGRAS2, and SmGRAS3, that either positively or negatively modulate tanshinone synthesis, comprehensive insights into GA's exact role remain scarce. Here, we provide an in-depth characterization of a bHLH TF, bHLH130. Overexpressing *bHLH130* markedly inhibited tanshinone synthesis, whereas its genetic knockout increased related metabolite yields. Yeast one-hybrid (Y1H), dual-luciferase (Dual-LUC), and electrophoretic mobility shift assays (EMSA) collectively confirmed that bHLH130 binds specifically to the E-box regions within the promoters of *DXS2*, *CPS1*, *KSL1*, and *CYP76AH1*, influencing their transcriptional activities. Additionally, protein interaction studies revealed a direct physical interaction between bHLH130 and DELLA4. Consequently, this research thoroughly explores and discusses the molecular pathways by which GA signaling utilizes bHLH130 to orchestrate the regulation of secondary metabolism. Clarifying the involvement of bHLH130 in diterpenoid metabolic flux greatly enhances the comprehension of interactions between GA signaling and tanshinone biosynthesis, providing essential insights for future metabolic engineering initiatives in *S. miltiorrhiza*.

2. Materials and methods

2.1. Plant materials and growth conditions

The *S. miltiorrhiza* hairy-root culture system[30] was utilized as previously described. Specifically, 0.2 g of fresh hairy roots were inoculated into sterile 100 mL triangular flasks containing 50 mL of hormone-free half-strength Murashige and Skoog liquid medium, followed by incubation in darkness at 25 °C on a rotary shaker at 110 rpm (Qiangwen, QWZY-C3, Taicang, China). GA_3 was prepared by dissolving it in ethanol at approximately 100 mmol/L, and the solution was sterilized through filtration with a 0.22 μm membrane. GA_3 treatments (final concentrations: ~50, 100, 150, and 200 μmol/L) were applied on day 18 after inoculation for 3 days. Control hairy roots were treated with pure ethanol. Samples were immediately frozen in liquid nitrogen and stored at −80 °C for RNA extraction.

2.2. Real-time quantitative PCR (RT-qPCR)

Hairy root samples were processed for RNA extraction utilizing an RNAprep Pure Plant Kit (TIANGEN, Beijing, China). The isolated RNA was subsequently reverse-transcribed into cDNA employing a PrimeScript™ RT reagent Kit (TaKaRa, Dalian, China). The integrity of RNA samples was verified *via* electrophoretic separation on 1.0% agarose gels, and their concentration was quantified with a micro-spectrophotometer (ALLSHENG, Hangzhou, China). Quantitative RT-PCR analyses were conducted on a QuantStudio™ 1 Real-Time PCR instrument (Applied Biosystems, Foster City, CA, USA) using SYBR Green PCR reagents from TaKaRa (Dalian, China). Primer sequences utilized in these assays are provided in Supporting Information Table S1. *Actin* was chosen as the endogenous control gene to standardize gene expression levels. The thermocycling profile involved an initial 30 s denaturation at 95 °C, then 40 repeated cycles each consisting of denaturation at 95 °C for 5 s and annealing/extension at 58 °C for 30 s. The relative abundance of target transcripts was quantified by employing the comparative $2^{-\Delta\Delta Ct}$ method[31].

2.3. Molecular cloning and bioinformatic analysis

Open reading frames (ORFs) encoding *bHLH130* and *DELLA* proteins were amplified by PCR with gene-specific primers listed in Table S1, then inserted into the entry cloning vector pGP-B2E[32]. The conserved structural domains were identified using NCBI's Conserved Domain Database. Additionally, sequence alignments were performed between the bHLH130 protein sequence from *S. miltiorrhiza* and selected bHLH sequences from *A. thaliana*. MEGA 11 software was used to construct a neighbor-joining phylogenetic tree, incorporating 1000 bootstrap replications for statistical robustness.

2.4. Yeast one-hybrid assay (Y1H)

The promoter regions containing tandem repeats of E-box motifs (*DXS2pro*, *CPS1pro*, *KSL1pro*, *CYP76AH1pro*) were cloned into the pAbAi vector, generating respective bait constructs. These constructs were introduced into Y1HGold yeast strains to develop bait strains, and the minimal inhibitory concentrations for Aureobasidin A (AbA) were optimized on selective SD/-Ura medium with AbA concentrations ranging from 150 to 800 ng/mL. The *bHLH130* CDS was inserted into the prey vector pGADT7. The transformed yeast cells were selected and cultured on SD/-Ura plates supplemented with AbA for 3−4 days at 29 °C.

2.5. Yeast two-hybrid assays (Y2H)

The full-length cDNA sequences of *bHLH130* and *DELLA* derived from *S. miltiorrhiza* were cloned into pGBKT7 and pGADT7 plasmids, respectively, using In-Fusion cloning technology. Subsequent yeast two-hybrid assays were implemented following the manufacturer's recommended guidelines (Clontech, Beijing, China).

2.6. Bimolecular fluorescence complementation (BiFC) and subcellular localization

Full-length *bHLH130* and *DELLA4* genes were subcloned into vectors (063075-DEST, 063076-DEST, and pGWB506) to generate YFP^N-*bHLH130*. YFP^C-*DELLA4*, *bHLH130*-GFP, and *DELLA4*-GFP. *Agrobacterium* strain GV3101 (OD_{600} = 0.6) infiltrated tobacco leaves (*Nicotiana benthamiana*). Fluorescence was visualized using a Leica TCS SP5 confocal microscope 3 days after infiltration.

2.7. Co-immunoprecipitation

Tobacco leaves infiltrated to express fusion proteins bHLH130-FLAG and Myc-DELLA4 were harvested three days post-infiltration. Total soluble proteins were isolated and subjected to immunoprecipitation using anti-FLAG agarose beads, followed by

analysis *via* SDS-PAGE and immunoblot assays utilizing anti-FLAG and anti-Myc antibodies.

2.8. Tanshinones extraction and HPLC analysis

Hairy roots were dried at 45 °C, ground, and 20 mg samples extracted with 70% methanol overnight. Extracts underwent ultrasonic shaking (45 min), centrifugation (9391×*g*, 10 min), and filtration (0.45 μm membrane). HPLC analysis followed previously described methods[33].

2.9. Luciferase assays

Promoter sequences of the genes *DXS2*, *CPS1*, *KSL1*, and *CYP76AH1* were amplified and ligated into the reporter vector pGreenII 0800-LUC. Effector constructs were generated by cloning *bHLH130* and *DELLA4* CDS into the pGreenII 62-SK vector. These recombinant vectors were introduced into *Agrobacterium* tumefaciens strain GV3101. Mixed bacterial suspensions were infiltrated into tobacco leaves, which were subsequently grown under greenhouse conditions for an additional three days. Luciferase activities were quantified using a dual-luciferase assay system (Yeasen, Shanghai, China) with a Varioskan™ LUX multimode microplate reader (Thermo, Waltham, USA). Visualization of fluorescence signals was achieved using a chemiluminescent imaging system (CLINX, Shanghai, China).

2.10. Electrophoretic mobility shift assay (EMSA)

The CDS of *bHLH130* was amplified *via* PCR using specialized primers and subsequently ligated into the pET-32a vector to produce recombinant proteins. The resulting plasmids were then transformed into *Escherichia coli* strain BL21 (DE3). Recombinant bHLH130 proteins fused with a His-tag were expressed and purified through Ni-NTA affinity chromatography. Synthetic DNA probes containing wild-type and mutant E-box motifs, as detailed in Table S1, were synthesized chemically. EMSA experiments were conducted using the LightShift Chemiluminescent EMSA Kit (Thermo, Waltham, USA). Following incubation at 25 °C for 30 min, protein-DNA complexes were separated using PAGE, and the results were visualized through chemiluminescent imaging.

2.11. Protein interaction predication

The amino acid sequences of bHLH130 and DELLA proteins were used as inputs for protein complex modeling. Protein complexes were predicted using AlphaFold3-Multimer[34] *via* the ColabFold platform and the AlphaFold3_mmseqs2 notebook with default parameters. Interface residues between bHLH130 and DELLA4 were identified using the "InterfaceResidues" PyMOL script.

2.12. Generation of transgenic hairy roots

For overexpression constructs, CDS of *bHLH130* and *DELLA4* were cloned into binary vectors 35S: 3 × FLAG and 35S: 5 × Myc, respectively. To generate the co-expression vector, the 35S:5 × Myc-*DELLA4*-NOS cassette was subcloned into the 35S:*bHLH130*-3 × FLAG binary vector. The CRISPR/Cas9 gene-editing vector was constructed by designing sgRNA for the *bHLH130* DNA sequence using the CRISPR-GE online tool[35]. Complementary oligo pairs synthesized by Tsingke Biotech (Hangzhou, China) were annealed to form sgRNA and inserted into the pHEE401E vector[36]. Vectors were individually transformed into *S. miltiorrhiza via Agrobacterium* rhizogenes strain ATCC15834 to produce transgenic hairy roots.

2.13. Protein extraction and cell-free degradation

Tobacco leaves transiently expressing Myc-tagged DELLA4 proteins were harvested, rapidly frozen, and pulverized in liquid nitrogen. In certain experiments, plants were pretreated with 50 μmol/L paclobutrazol for six days (applied once every three days, twice in total) before the expression of Myc-DELLA4 constructs. Protein was extracted using degradation buffer (25 mmol/L Tris−HCl pH 7.5, 10 mmol/L NaCl, 10 mmol/L $MgCl_2$, 4 mmol/L PMSF, 5 mmol/L DTT, 10 mmol/L ATP) and clarified twice *via* centrifugation at 15,000×*g* at 4 °C for 10 min[37]. Extracted proteins were evenly divided and incubated in the presence or absence of proteasome inhibitor MG132 (or equivalent volumes of DMSO as control). Reactions proceeded at 22 °C, with samples collected at designated time points. Western blotting (WB) was subsequently performed to evaluate DELLA protein stability.

3. Results

3.1. Transcriptomic analysis identifies bHLH130 as a GA-responsive gene in hairy roots

Previous studies have shown that exogenous application of GA enhances the accumulation of tanshinones[29]. To thoroughly characterize the genes responsive to GA treatment, we performed RNA-seq analysis on hairy root samples subjected to GA exposure and untreated controls (CK). Differentially expressed genes (DEGs) were screened using stringent criteria of $|\log2 \text{ fold change (FC)}| \geq 1$ and statistical significance of $P < 0.05$, resulting in the identification of 4280 DEGs, which are depicted in the volcano plot (Fig. 1A). Among these identified genes, 1882 were significantly induced, whereas 2398 were significantly suppressed in GA-treated groups relative to control samples. Gene Ontology (GO) enrichment analysis identified "Catalytic activity", "Membrane", and "Response to stimulus" as the most significantly represented functional categories (Fig. 1B). Furthermore, the Kyoto Encyclopedia of Genes and Genomes (KEGG) enrichment results highlighted marked enrichment in categories associated with "Metabolic pathways", "Biosynthesis of secondary metabolites", and "Plant hormone signal transduction" (Fig. 1C).

Subsequently, expression patterns of several key genes associated with tanshinone synthesis were evaluated following GA treatment. Specifically, seven critical biosynthetic genes, including *DXS2*, *GGPPS*, *KSL1*, and *CYP76AH1*, exhibited significantly elevated transcript levels in GA-treated hairy roots (Fig. 1D). These genes are directly involved in tanshinone biosynthesis[10]. Further transcriptomic analysis identified potential regulatory factors modulating tanshinone biosynthesis in response to GA. Expression levels increased for 237 TF-encoding genes, whereas 112 TF-encoding genes exhibited decreased expression (Table S1). Notably, *bHLH130*, orthologous to Arabidopsis *bHLH130*, displayed significant downregulation (Supporting Information Fig. S1A. RT-qPCR confirmed this significant repression of *bHLH130* expression following GA treatment (Fig. S1B). We then assessed whether *bHLH130* expression depended on GA concentration. 18-day-old hairy roots were treated with various GA concentrations (0, 50, 100, and 150 μmol/L) for 3 days.

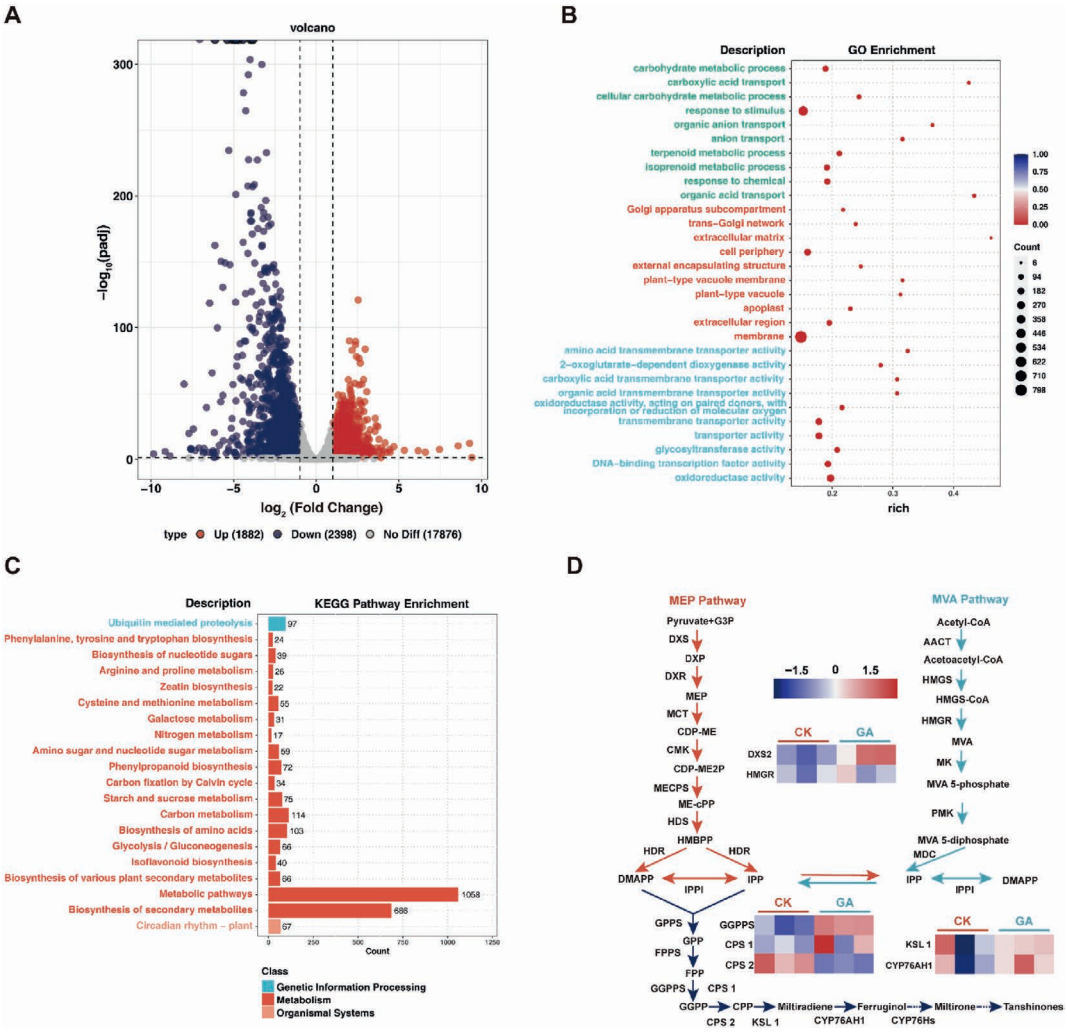

Figure 1 Transcriptomic profiling of GA-treated hairy roots in *S. miltiorrhiza*. (A) Volcano plot of DEGs between GA-treated and CK hairy roots; (B) GO classification of DEGs between GA-treated and CK hairy roots; (C) KEGG enrichment analysis of DEGs between GA-treated and CK hairy roots; (D) Expression patterns of key tanshinone biosynthetic genes under GA treatment.

bHLH130 transcript levels decreased in a dose-dependent manner (Fig. 2A). These results indicate a crucial role for *bHLH130* in the GA signaling pathway.

3.2. *Characterization and subcellular localization of bHLH130*

The coding sequence of *bHLH130* was amplified from *S. miltiorrhiza* to facilitate the characterization of this gene. Analysis revealed that *bHLH130* possesses an ORF spanning 1188 bp, which encodes a predicted polypeptide consisting of 395 amino acids. To better understand the physiological relevance of *bHLH130*, its transcript abundance was quantified across different tissues *via* RT-qPCR. Expression analysis detected *bHLH130* in diverse plant organs, including flowers, stems, leaves, fibrous roots, root epidermis, and xylem. Notably, expression levels were highest in roots (root epidermis, xylem, and fibrous roots) and leaves (Fig. 2B). Since tanshinones accumulate and are synthesized primarily in roots, the high expression of *bHLH130* suggests its functional role in tanshinone biosynthesis.

Given that TFs are DNA-binding proteins that interact with the promoters of target genes and control their expression in the nucleus, we performed a subcellular localization assay to explore whether bHLH130 locates in nuclear. Thus, the *bHLH130* coding sequence was fused to a GFP reporter driven by the cauliflower mosaic virus 35S constitutive promoter, creating the fusion construct 35S:*bHLH130*-GFP. This construct was transiently introduced into tobacco leaves. Subsequent imaging by confocal microscopy revealed distinct nuclear accumulation of the fusion protein (bHLH130-GFP), in contrast to the even distribution observed for the control GFP protein (35S:GFP) alone (Fig. 2C).

To further confirm localization under physiological conditions, hairy roots of *S. miltiorrhiza* stably expressing the bHLH130-GFP fusion protein were generated. Consistent with transient assays, bHLH130-GFP was specifically localized to the nucleus (Fig. 2D), while negative control roots showed no detectable fluorescence (Fig. S1C). This result is consistent with the localization observed in the leaves of tobacco.

3.3. *bHLH130 negatively regulates tanshinone biosynthesis*

To elucidate the biological roles of *bHLH130*, stable hairy root lines (bHLH130^{OE}) overexpressing *bHLH130* driven by the 35S promoter were established in *S. miltiorrhiza*. Hairy root generated by *A. rhizogenes* strain ATCC15834 without plasmids served as

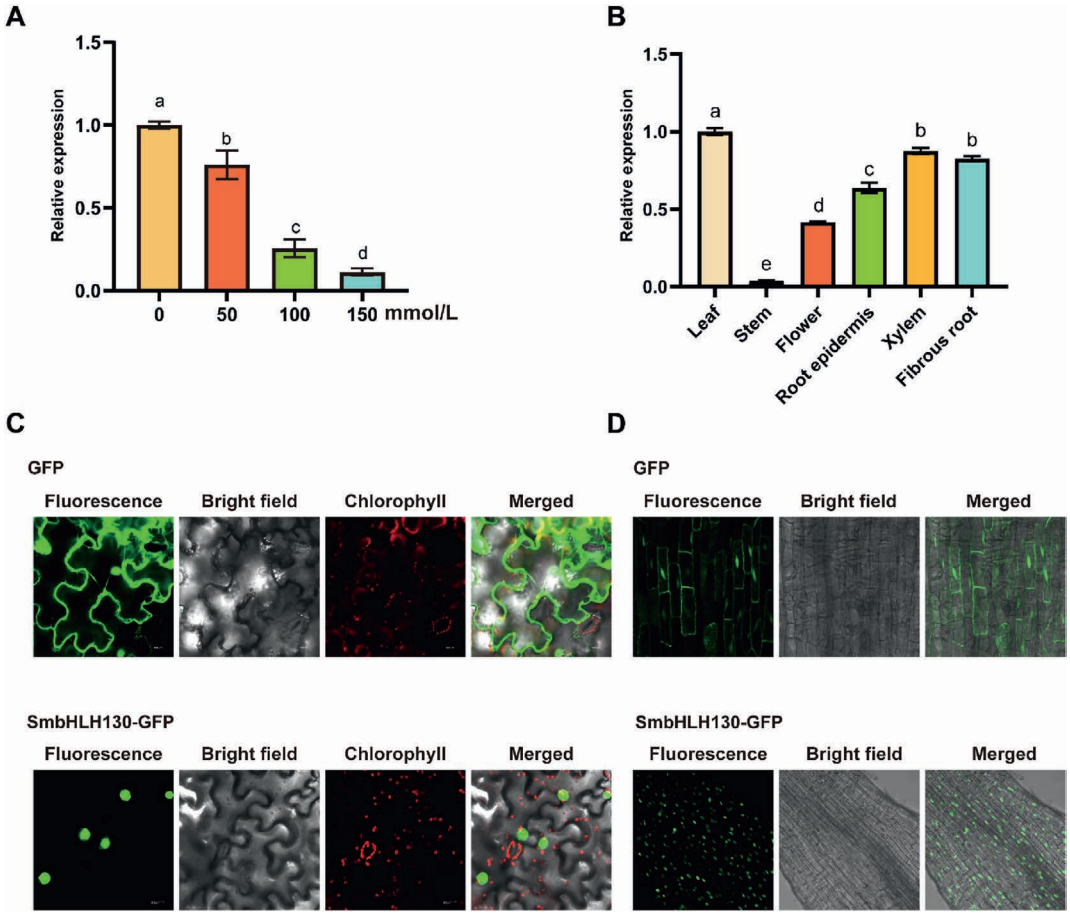

Figure 2 Expression patterns and subcellular localization of bHLH130. (A) RT-qPCR analysis of *bHLH130* expression in 18-day-old hairy roots treated with GA; *Actin* served as internal control; (B) Tissue-specific expression of *bHLH130* in leaves, stems, flowers, root epidermis, xylem, and fibrous roots of 2-year-old plants during flowering. Leaf expression was normalized to 1, with *Actin* as internal control; (C) Transient expression of *bHLH130*-GFP fusion protein in *N. benthamiana* leaves confirmed nuclear localization; (D) Stable expression of bHLH130-GFP fusion protein confirmed nuclear localization in *S. miltiorrhiza* hairy root cells. Data are presented as the mean ± SD ($n = 3$), with different letters indicating statistically significantly at $P < 0.05$ (one-way ANOVA).

control samples (CK). Positive transgenic hairy roots were validated through PCR analysis (Supporting Information Fig. S2). Three independent bHLH130^{OE} lines were selected for subsequent analyses. Expression of *bHLH130* significantly increased in transgenic lines compared with CK, although variation existed among independent lines (Fig. 3A).

Cryptotanshinone (CT), dihydrotanshinone I (DT-I), tanshinones I (T-I), and tanshinone IIA (T-IIA) are the predominant tanshinone constituents identified in *S. miltiorrhiza*. As indicated in Fig. 3B, substantial reductions were observed in CT, DT-I, T-I, and especially T-IIA concentrations within the bHLH130^{OE} transgenic hairy root lines. To further explore the role of *bHLH130*, we generated mutant lines (bHLH130^{KO}) using CRISPR-Cas9 gene editing technology (Fig. 3C). Knockout mutants displayed significantly increased tanshinone contents compared to CK (Fig. 3D). These results suggest that bHLH130 negatively regulates tanshinone accumulation.

3.4. bHLH130 directly binds promoters of tanshinone biosynthetic genes to repress their expression

To further clarify the regulatory influence of *bHLH130* on tanshinone biosynthetic processes, a transcriptomic analysis was undertaken comparing bHLH130^{OE} lines with CK plants. Employing stringent criteria ($|\log_2 FC| > 1$; $P < 0.05$), the analysis identified 5668 genes with altered expression patterns, comprising 3002 upregulated and 2666 downregulated transcripts (Fig. 4A). KEGG pathway enrichment analysis highlighted significant enrichment of differentially expressed genes within "Organismal Systems", "Genetic Information Processing", and "Metabolism" categories (Fig. 4B). Notably, several key genes crucial for tanshinone production, such as *DXS2*, *CPS1*, *KSL1*, and *CYP76AH1*, displayed significantly decreased transcriptional levels within bHLH130^{OE} hairy roots (Fig. 4C). These findings were further substantiated through RT-qPCR assays, demonstrating significant downregulation of these genes in bHLH130^{OE} roots (Fig. 5A) and upregulation in bHLH130^{KO} lines (Fig. 5B), consistent with the RNA-seq data.

It is widely acknowledged that bHLH transcription factors exert their regulatory effects by directly interacting with specific DNA elements, typically canonical G-box (CACGTG) or E-box (CANNTG with N = A, T, G, C) sequences[38]. Therefore, we analyzed the promoter sequences of these genes and found that all four promoters contain the E-box motif. Subsequently, Y1H assays determined whether bHLH130 directly binds to the promoters of *DXS2*, *CPS1*, *KSL1*, and *CYP76AH1 in vitro*. Promoter

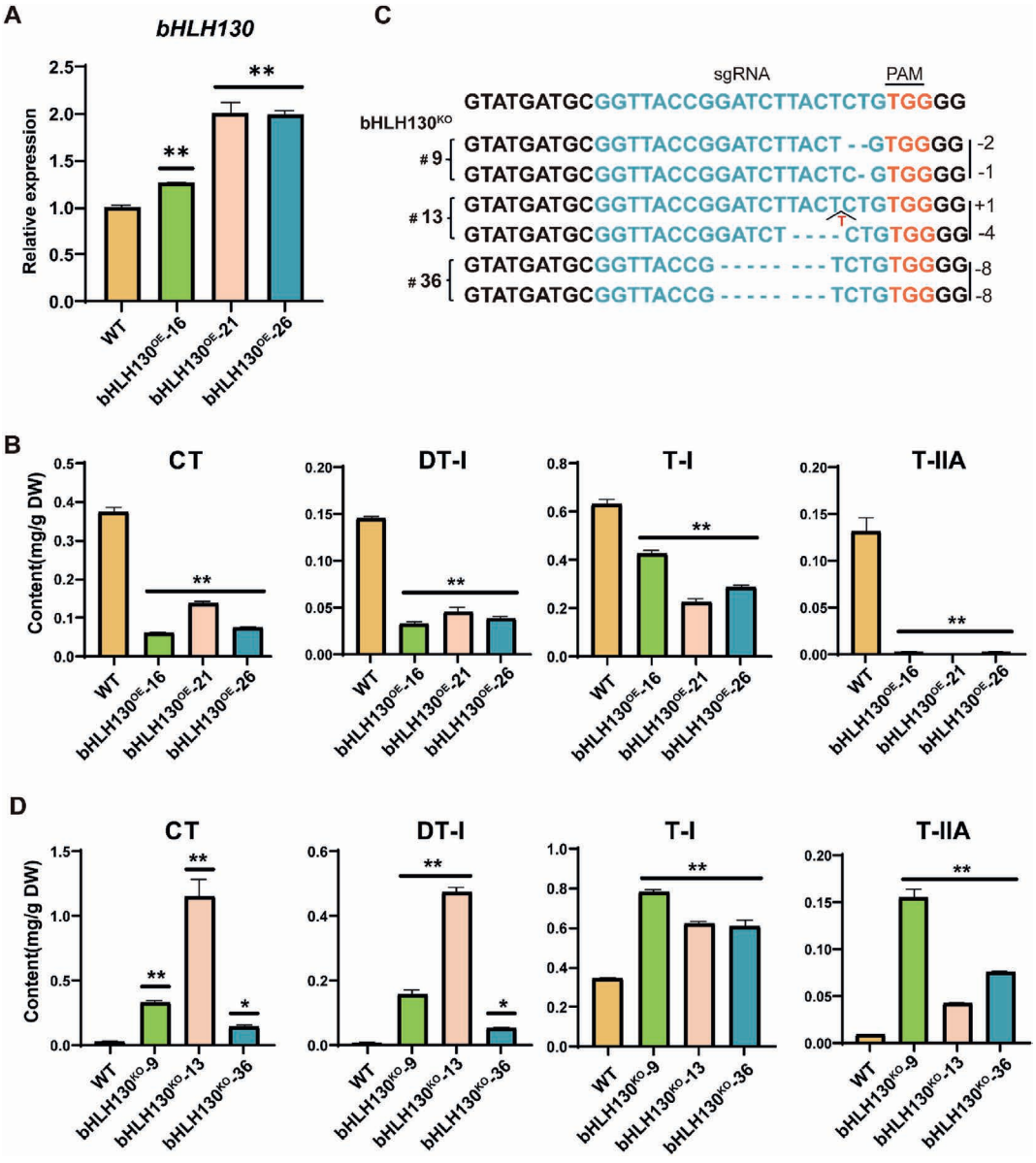

Figure 3 Overexpression and knockout of *bHLH130* affect tanshinone accumulation in hairy roots. (A, C) HPLC quantification of CT, DT-I, T-I, and T-IIA contents in hairy roots; (B, D) Genomic DNA sequences of *bHLH130* knockout (bHLH130^{KO}) lines; original sequence shown at top. Statistical significance determined by Student's *t*-test. *$P < 0.1$, **$P < 0.01$, data are presented as the mean ± SD.

fragments (*DXS2pro*, *CPS1pro*, *KSL1pro*, and *CYP76AH1pro*) were integrated separately into Y1HGold yeast cells. After introducing the pGADT7-*bHLH130* plasmid, all strains carrying target promoters grew on selective media (Fig. 6A). We then performed an EMSA assay to further verify whether bHLH130 binds to the promoters of *DXS2*, *CPS1*, *KSL1*, and *CYP76AH1*. His-tagged bHLH130 protein (bHLH130-His) and labeled DNA probes containing E-box motifs revealed clear protein−DNA complexes band. Competition assays with unlabeled probes confirmed specificity (Fig. 6B). These results provide strong evidence confirming that bHLH130 binds to the native promoters of at least four tanshinone biosynthetic genes.

Subsequently, we examined whether bHLH130 repressed the transcription of four tanshinone biosynthetic genes using a dual transactivation luciferase system (LUC/REN) in tobacco leaves. Promoter fragments driving LUC (*DXS2pro:LUC*, *CPS1pro:LUC*, *KSL1pro:LUC*, *CYP76AH1pro:LUC*) were co-expressed with *bHLH130* (35S promoter-driven effector). Co-expression with *bHLH130* resulted in significant repression of luciferase activity compared with controls (Fig. 6C and D). These results demonstrate that bHLH130 negatively regulates tanshinone biosynthesis by directly binding and repressing these target genes.

3.5. bHLH130 interacts closely with the GA-signaling repressor DELLA

Previous experiments demonstrated that GA suppresses *bHLH130*, suggesting its potential involvement in the GA signaling pathway. To test this hypothesis, AlphaFold3 predicted the interaction potential between bHLH130 and DELLA proteins. The predicted bHLH130−DELLA4 complex showed a higher interface-predicted TM score (ipTM = 0.66) compared to complexes

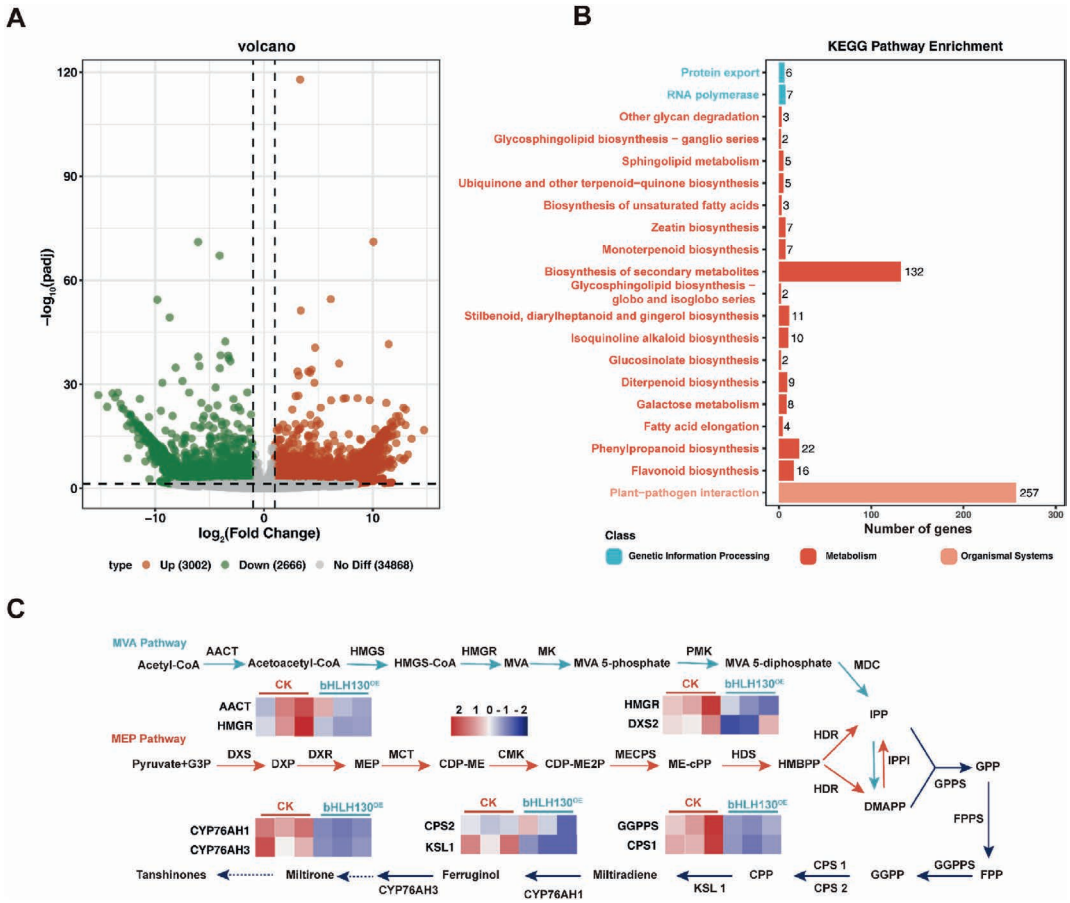

Figure 4 Transcriptome analysis indicates *bHLH130* regulates tanshinone pathway genes. (A) Volcano plot of DEGs between CK and bHLH130^{OE} hairy roots; (B) KEGG classification of DEGs; (C) Heatmap illustrating expression fold-changes (log_2FC) of tanshinone biosynthesis-related genes in bHLH130^{OE} lines relative to CK.

involving DELLA1 (0.24), DELLA2 (0.28), and DELLA3 (0.45). This indicates that bHLH130 may preferentially form complexes with DELLA4 (Fig. 7A). Furthermore, the analysis of bHLH130−DELLA4 complex exhibits that bHLH130 Ala-223 forms two H-bonds with Glu-234 and Try-235 of DELLA4, and bHLH130 Gln-303 forms another H-bond with Glu-88 of DELLA4 (Fig. 7A). Previous research has reported that the C-terminal of DELLA is responsible for interacting with the C-terminal of bHLH130 *via* Y2H assay[39]. Therefore, in the bHLH130−DELLA4 complex, bHLH130 Ala-223, Gln-303 and Glu-234, and Try-235 of DELLA may form the core interaction interface.

Furthermore, Y2H experiments were also employed to verify protein−protein interactions between DELLA family members and bHLH130. Strong activation of the reporter genes *MEL1*, *ADE2*, *HIS3*, and *lacZ* was detected in yeast strains simultaneously expressing *bHLH130* and *DELLA4*, as indicated by distinct blue colony formation on selective SD medium lacking Ade, His, Leu, and Trp but supplemented with X-α-Gal (Fig. 7B). On the other hand, DELLA2 exhibited only weak interaction with bHLH130, and interactions involving DELLA1 and DELLA3 were almost undetectable (Supporting Information Fig. S3). To further validate the interactions between bHLH130 and DELLA4 protein *in vivo*, Co-IP assays verified the interaction between bHLH130 and DELLA4 in plant tissues. Transient co-expression assays conducted in tobacco leaves expressing bHLH130-FLAG and Myc-DELLA4 fusion proteins demonstrated successful co-precipitation of Myc-DELLA4 using anti-FLAG antibodies magnetic beads (Fig. 7C). Finally, the BiFC assay results revealed pronounced fluorescent signals localized specifically within nuclei of tobacco leaf cells transiently co-expressing YFP^{C}-bHLH130 and YFP^{N}-DELLA4 fusion proteins (Fig. 7D). Collectively, these data provide compelling evidence for the specific interaction between bHLH130 and DELLA4 *in vivo*.

3.6. DELLA4 attenuates the inhibitory effect of bHLH130 on tanshinones biosynthesis

To determine whether the interaction between bHLH130 and DELLA4 influences the regulation of bHLH130 target genes, *KSL1* was selected as a representative target gene for dual-LUC assays. The results indicated that bHLH130 significantly repressed *KSL1* expression, but this repression was attenuated upon co-expression of *DELLA4*(Fig. 8A). Furthermore, we also generated DELLA4-overexpressing (DELLA4^{OE}) and bHLH130-DELLA4 co-overexpressing (DELLA4+bHLH130^{OE}) hairy roots to explore whether DELLA4 impedes the function of bHLH130 in tanshinone biosynthesis. Quantification showed significantly increased tanshinone levels (CT, DT-I, T-I, T-IIA) in DELLA4^{OE} lines. However, tanshinone contents remained unchanged relative to control when *bHLH130* and *DELLA4* were co-overexpressed (Fig. 8B). These findings suggest that DELLA4

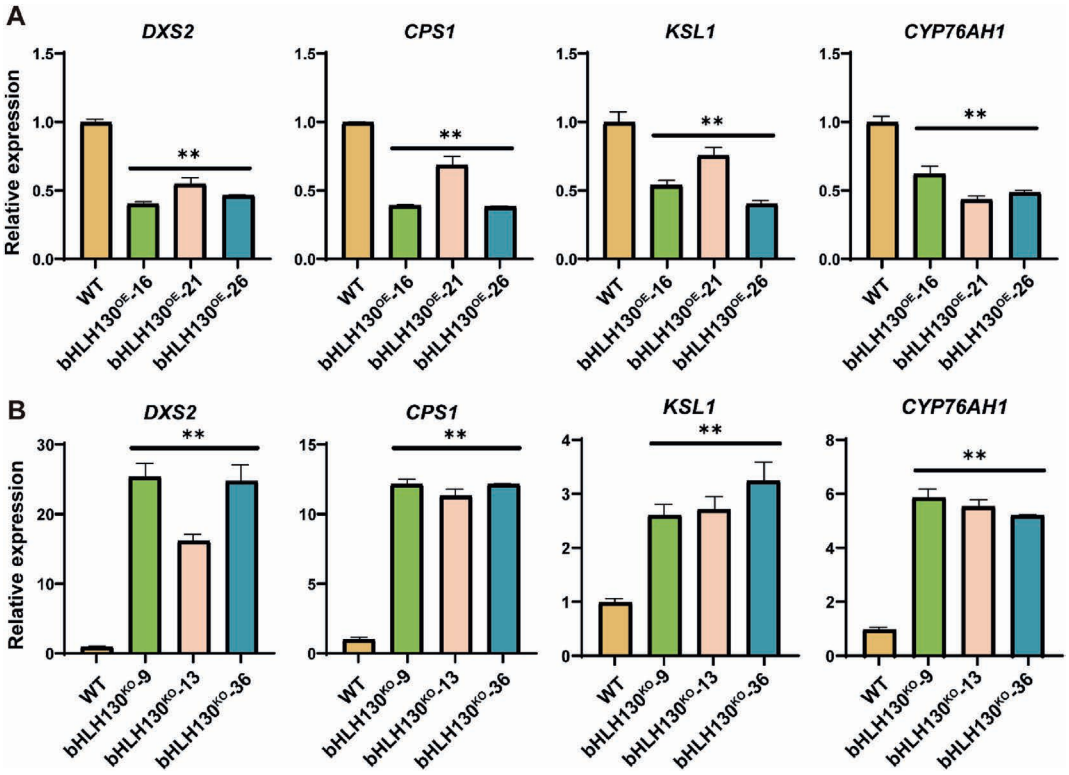

Figure 5 Expression of key tanshinone biosynthetic genes in transgenic hairy roots. (A) Expression levels in bHLH130^{OE} hairy roots; (B) Expression levels in bHLH130^{KO} hairy roots. $^{**}P < 0.01$, data are presented as the mean ± SD.

binds bHLH130, thereby diminishing its repressive effect on tanshinone biosynthesis genes and promoting metabolite accumulation.

Since DELLA proteins act as negative regulators in the GA pathway and undergo GA-mediated degradation, we conducted a series of assay to investigate whether DELLA4 degradation depends on GA. Firstly, we investigated whether DELLA4 degradation *via* the ubiquitin-26S proteasome system. To this end, a cell-free system was conducted to explore the degradation rate of myc-DELLA4 in the presence or absence of the proteasome inhibitor MG132. Western bolt assay showed that the Myc-DELLA4 protein degraded rapidly in absence of MG132, while degradation was significantly delayed in its presence (Fig. 8C). These results indicate that DELLA4 can be degraded by the 26S proteasome. Subsequently, we investigated whether this degradation process requires GA. Tobacco leaves were pretreated with paclobutrazol to inhibit endogenous GA biosynthesis prior to the transient expression of DELLA4. As shown in Fig. 8C, paclobutrazol inhibited SmDELLA4 degradation, confirming that its degradation depends on GA.

4. Discussion

Plants widely synthesize terpenoids, and their biosynthesis is influenced considerably by various biotic and abiotic environmental stress factors, affecting both crop productivity and nutritional quality[40,41]. Additionally, due to their distinct chemical attributes, terpenoids are extensively utilized by pharmaceutical industries for medicinal applications. Tanshinones, diterpenoid compounds predominantly isolated from the herb *S. miltiorrhiza*, have long been employed in treating cerebrovascular and cardiovascular diseases. However, as typical for many bioactive natural products, tanshinones inherently accumulate at relatively low concentrations in plant tissues. Previous reports have demonstrated that exogenous GA application significantly stimulates tanshinone production in *S. miltiorrhiza*[29,42], although the precise underlying molecular mechanisms were not fully elucidated. This study identified the GA-responsive TF bHLH130 as a negative regulator of tanshinone synthesis, directly interacting with promoters of key genes involved in the tanshinone biosynthetic pathway. Moreover, bHLH130 physically associates with DELLA4, a recognized repressor in GA signal transduction.

4.1. *bHLH130 acts as a negative regulator of tanshinone biosynthesis*

Plant secondary metabolite biosynthesis is governed by complex regulatory pathways at transcriptional, post-transcriptional, translational, post-translational, and chromatin levels. Transcriptional regulation, the initial step in the flow of information from genome to proteome, critically determines secondary metabolite accumulation[43]. Both academic and commercial interests have driven extensive research to elucidate how TFs orchestrate secondary metabolite production. Belonging to one of the most abundant groups of plant TFs family, bHLH proteins are widely conserved among eukaryotes. These TFs act either as repressors or activators essential for plant responses to environmental stimuli, as well as developmental and growth-related processes[38]. In addition, bHLH TFs are recognized as key regulators influencing secondary metabolism pathways across numerous medicinal plant species, notably *Artemisia annua* and *S. miltiorrhiza*[21,44,45]. In *A. annua*, AabHLH1 directly activates expression of *AaADS* and

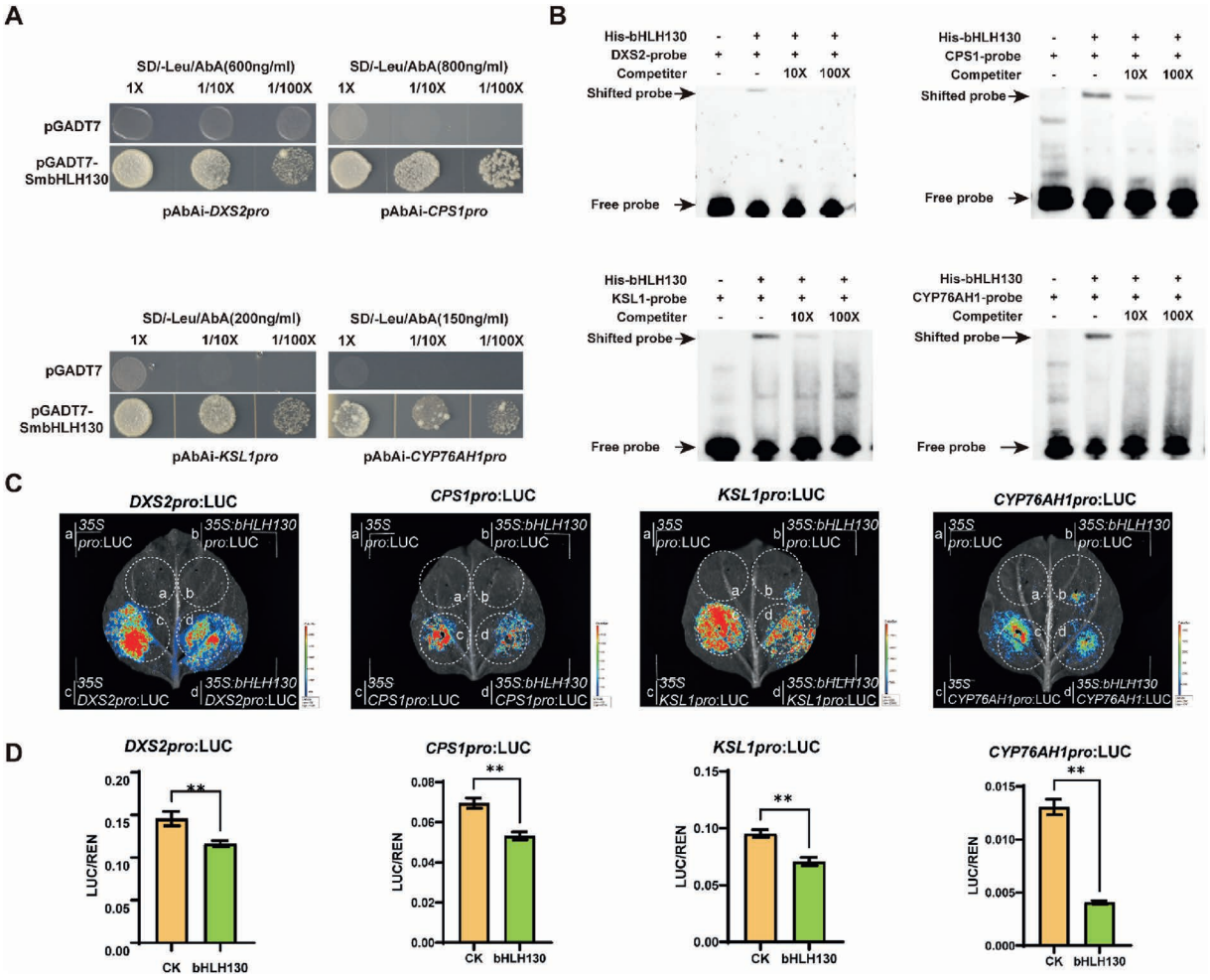

Figure 6 bHLH130 binds to E-boxes in tanshinone biosynthetic gene promoters and represses their transcription. (A) Y1H assays confirmed binding of bHLH130 to E-box motifs in *DXS2*, *CPS1*, *KSL1*, and *CYP76AH1* promoters; (B) EMSA verified specific binding of bHLH130 to promoter fragments; (C) Luciferase imaging (LUC) captured three days post-infiltration; (D) LUC assays showed bHLH130 significantly repressed transcription of *DXS2*, *CPS1*, *KSL1*, and *CYP76AH1* promoters (relative LUC activity normalized to REN luciferase). $^{**}P < 0.01$, data are presented as the mean ± SD.

AaCYP71AV1, consequently enhancing artemisinin biosynthesis[44]. Several distinct bHLH TFs have also been identified from *S. miltiorrhiza*. Among these, SmbHLH37 positively impacts salvianolic acid B accumulation by directly interacting with the promoters of *SmTAT1* and *SmPAL1*, thereby activating their transcription[46]. SmbHLH59 activates tanshinone and phenolic acid biosynthesis by binding E/G-box motifs in pathway gene promoters; however, this activation is inhibited by interactions with JAZ1 and JAZ8[47]. Previously, we demonstrated that overexpression of *bHLH10* enhances tanshinone biosynthesis[21]. Collectively, these studies indicate that bHLHs predominantly act as positive regulators of bioactive compound biosynthesis. However, in this research, we wandered whether bHLH negatively regulate tanshinone biosynthesis. GA treatment increased tanshinone levels in hairy roots, and DEG analysis identified *bHLH130*, significantly downregulated in GA-treated hairy roots (Figs. 1 and 2). In addition, the apple homologous gene *MdbHLH130* was reported negatively regulated the flavonoid biosynthesis[48]. Prompted by these findings, we further examined the hypothesis that *bHLH1*30 might negatively modulate tanshinone production. Subsequent molecular and genetic investigations substantiated this hypothesis, demonstrating conclusively that *bHLH130* acts as a repressor of tanshinone synthesis.

It is increasingly acknowledged that the physical clustering of specialized metabolite biosynthetic genes is not exclusive to microbial organisms. An expanding number of biosynthetic gene clusters in plants have been reported, frequently exhibiting coordinated regulatory patterns reported[49,50]. Such clusters typically display synchronized transcriptional responses when subjected to external hormones or environmental stressors, both biotic and abiotic. Consequently, unknown biosynthetic genes in one cluster can be predicted through co-expression analysis across tissues, developmental stages, and stress treatments[51]. Previous studies identified *CPS1*, *KSL1*, and *CYP76AH1* within a large tanshinone biosynthetic gene cluster on chromosome 6 of *S. miltiorrhiza*[14]. CPS1 and KSL1 participate in synthesizing the abietane-type diterpene miltiradiene, a potential intermediate in tanshinone biosynthesis. Subsequently, CYP76AH1 oxidizes miltiradiene into ferruginol, forming a critical branching point in the pathway[13]. Several reports indicate that the upstream MEP-pathway gene *DXS2* typically acts synergistically with *CPS1* during tanshinone

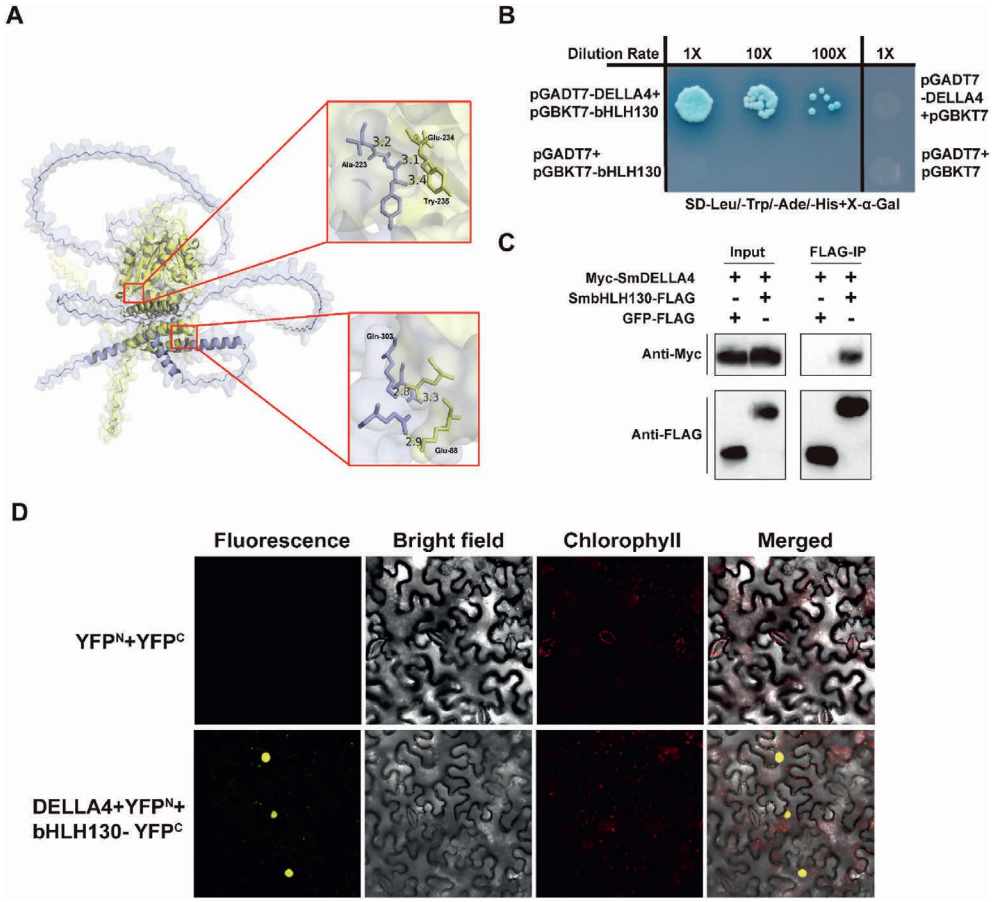

Figure 7 Interaction between bHLH130 and DELLA4. (A) AlphaFold3-predicted structure of the bHLH130 (purple)−DELLA4 (yellow) complex, with interface-predicted TM score (ipTM); (B) Y2H assays confirming interaction between bHLH130 and DELLA4; (C) Co-IP assay verifying interaction of bHLH130 with DELLA4; (D) BiFC assay demonstrating interaction between bHLH130 and DELLA4.

biosynthesis[20,52,53], suggesting coordinated regulation by a common TF. In our study, we demonstrated that bHLH130 coordinately regulates *DXS2*, *CPS1*, and other key genes (*HMGR*, *CYP76AH1*, and *CYP76AH*, Fig. 4C). Nevertheless, results from *in vitro* and *in vivo* assays indicated that bHLH130 only directly associates with E-box sequences in the promoter regions of four key tanshinone biosynthesis genes (*DXS2*, *CPS1*, *KSL1*, *CYP76AH1*). This indicates that these genes are directly regulated by bHLH130, while *HMGR* and *CYP76AH3* may be regulated indirectly by this TF (Fig. 6). Recent research has shown that bHLH51 interacts with MYB111 and TTG1 to form a MYB-bHLH-WD40 (MBW) complex, which regulates the accumulation of phenolic acids and tanshinones in *S. miltiorrhiza*[54]. Furthermore, the MBW complex in *A. thaliana* also plays a crucial role in pectin biosynthesis[55]. These findings suggest that bHLH130 may also participate in regulating the expression of *HMGR* and *CYP76AH3* by forming its own MBW complex. Future research should aim to identify additional TFs that interact with bHLH130 to explore the molecular mechanisms underlying its role in regulating tanshinone biosynthesis. Take together, the comprehensive genetic, molecular, and biochemical evidence, it is reasonable to propose that bHLH130 can directly binds to the *cis*-elements of the three genes within the tanshinone biosynthetic gene cluster and one gene (*DXS2*) in MEP pathway, thereby negatively regulating tanshinone biosynthesis (Figs. 4C and 6A, and B).

4.2. GA exhibits dual roles in tanshinone biosynthesis

GA, an essential plant hormone, orchestrates diverse biological processes, including seed germination, floral induction, stem elongation, and seed maturation[22]. Depending upon the plant species, specific tissue contexts, and GA dosage, GA can either stimulate or inhibit secondary metabolite biosynthesis. For instance, GA application markedly elevates anthocyanin content and PAL activity in apples, whereas in litchi (*Litchi chinensis*), GA exposure significantly suppresses biosynthetic genes such as *PAL*, *C4H*, *CHS*, and *UFGT* [56]. Previously, it was shown that external GA treatment enhances tanshinone production in *S. miltiorrhiza* by elevating transcript levels of genes such as *CPS1* and *KSL1*[29,42]. In contrast, our current results revealed the down-regulation of *CPS1* and *KSL1* by bHLH130, suggesting a hypothesis wherein GA might enhance tanshinone biosynthesis by suppressing *bHLH130* expression. It is well established that the biosynthesis of plant secondary metabolites under normal growth conditions incurs ecological costs and may adversely affect plant growth[57]. Although it remains unclear whether excessive tanshinone accumulation harms *S. miltiorrhiza* roots, recent research indicates cytotoxic effects of tanshinone IIA on *A. thaliana* roots. Additionally, tanshinones can be exported from peridermal cells into the soil *via* the ABC transporter SmABCG1[58]. Thus, it is plausible that *S. miltiorrhiza* evolved mechanisms to limit

excessive tanshinone production in response to complex and changing environment.

DELLA proteins function as key repressors in GA signaling. Initially, GA binds the receptor GID1, causing a conformational change. This facilitates binding and complex formation with DELLA proteins, which are subsequently degraded *via* the ubiquitin−proteasome pathway. This degradation releases transcriptional inhibition, activating downstream GA-responsive genes[28,59,60]. Moreover, DELLA proteins can interact with bHLH TFs, inhibiting their transcriptional activity. Experimental evidence indicates DELLA proteins directly bind MYC2, impairing its DNA-binding capability and affecting volatile sesquiterpene biosynthesis in *A. thaliana*[59,61]. *S. miltiorrhiza* contains four DELLA proteins[25]. Our study demonstrated that DELLA4 degradation depends on GA and interacts with bHLH130 (Figs. 7 and 8C), suggesting that bHLH130 regulates tanshinone biosynthesis *via* the GA-DELLA signaling pathway. To further investigate the molecular mechanisms underlying this interaction, we performed Dual-LUC assays to assess the effects of DELLA4 and bHLH130 on *KSL1*. Results indicated that bHLH130 represses *KSL1* expression, but this repression is reduced upon co-expression with *DELLA4* (Fig. 8A). Moreover, we generated DELLA4^{OE} and DELLA4+bHLH130^{OE} co-expressing hairy roots to explore whether DELLA4 impedes the function of bHLH130 in tanshinone biosynthesis. Quantification of tanshinones demonstrated that the DELLA4^{OE} lines significantly increased levels of CT, DT-I, T-I, and T-IIA. In contrast, when *DELLA4* and *bHLH130* were co-overexpressed, the levels of tanshinones did not significantly change compared to CK (Fig. 8B). These results suggest that when *DELLA4* is overexpressed, it will bind more bHLH130, thereby disrupting the function of bHLH130 and enhancing tanshinone biosynthesis. Conversely, in the case of co-overexpression of *DELLA4* and *bHLH130*, despite the elevation of bHLH130 protein levels, it remains bound by the concurrently increased DELLA4 protein. Consequently, the levels of tanshinones in the DELLA4+bHLH130^{OE} lines did not significantly change compared to CK. Based on these results, we propose a regulatory model outlining the relationship between GA signaling and the biosynthesis of tanshinones: under GA-deficient conditions, DELLA proteins physically interact with and possibly sequester bHLH130, while other transcription factors mediate gene expression within the tanshinone biosynthetic route. However, in the presence of GA, transcription of *bHLH130* is repressed, diminishing its suppressive impact and thus facilitating elevated tanshinone production. Simultaneously, GA triggers DELLA protein degradation through proteasome-mediated pathways, releasing bHLH130. Consequently, free bHLH130 represses the transcription of critical tanshinone biosynthetic genes, such as *DXS2*, *CPS1*, *KSL1*, and *CYP76AH1*, ultimately inhibiting tanshinone biosynthesis. Through this multiple regulatory mechanism, the accumulation of tanshinones is kept in check, preventing adverse effects on

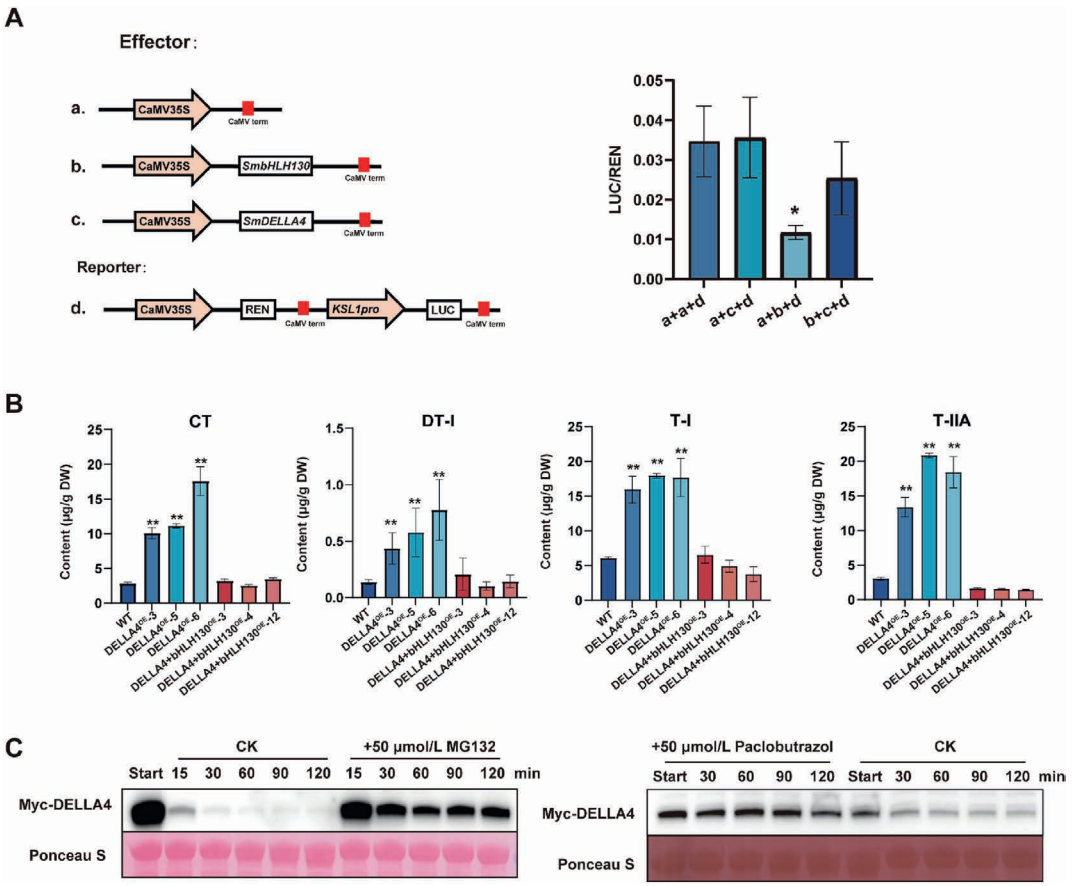

Figure 8 DELLA4 reduces the inhibitory effect of bHLH130 on tanshinones biosynthesis. (A) DELLA4 attenuates the transcriptional repression activity of bHLH130 on the *KSL1* promoter. (B) Quantification of tanshinones in DELLA4^{OE} and DELLA4+bHLH130^{OE} hairy roots. (C) Effects of MG132 and GA on DELLA4 protein degradation in the cell free assay. $^{*}P < 0.1$, $^{**}P < 0.01$, data are presented as the mean ± SD.

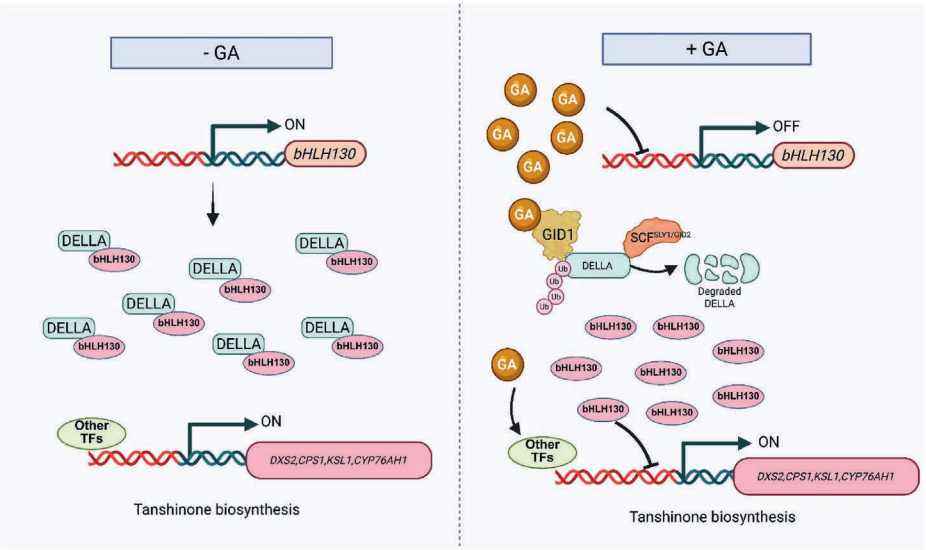

Figure 9 Hypothetical model illustrating the role of *bHLH130* in mediating tanshinone biosynthesis in *S. miltiorrhiza*. In the absence of GA, DELLA proteins interact with bHLH130, while other TFs regulate tanshinone biosynthesis. GA presence suppresses *bHLH130* expression, promoting tanshinone biosynthesis. However, GA also facilitates DELLA protein degradation *via* the 26S proteasome, releasing bHLH130 to inhibit transcription of *DXS2*, *CPS1*, *KSL1*, and *CYP76AH1*, thereby repressing tanshinone production. Through this multiple regulatory mechanism, the accumulation of tanshinones is kept in check.

the normal growth of the plants. Meanwhile, these observations also underscore GA's complex regulatory function in modulating tanshinone production through intricate molecular interactions involving DELLA proteins and bHLH130 (Fig. 9).

5. Conclusions

This study identified and functionally characterized bHLH130, a GA-responsive TF that negatively regulates tanshinone biosynthesis in *S. miltiorrhiza* hairy roots. Molecular mechanism analyses indicate that bHLH130 directly regulates the expression of genes involved in the tanshinone pathway, including *DXS2*, *CPS1*, *KSL1*, and *CYP76AH1*, thereby repressing tanshinone production. Furthermore, we reveal that bHLH130 interacts with DELLA4 to participate in GA signal mediating the tanshinone biosynthesis accumulation. Collectively, these insights significantly expand our understanding of bHLH TFs and GA-related regulatory networks governing secondary metabolism in plants.

Acknowledgments

This work was supported by National Natural Science Foundation of China (Nos.: 82225047, 82304665, 82170274, and 82104325), National Key Research and Development Program of China (2022YFC3501703), Zhejiang Provincial Natural Science Foundation of China (LQ23H280016, LZ24H280003), Postdoctoral Fellowship Program of CPSF (GZC20233561, China), and Key project at central government level: the ability establishment of sustainable use for valuable Chinese medicine resources (2060302, China).

Author contributions

Haizheng Yu: Writing-original draft, methodology, funding acquisition. Haizheng Yu, Ruiyang Yao, Yongxing Chen, and Sixue Zhang: Investigation, data curation. Ruiyang Yao: Software. Bingcong Xing: Writing-review & editing. Wenrui Li andBingcong Xing: Methodology. Dongfeng Yang: Conceptualization, writing-review & editing. Lei Zhang: Conceptualization, writing-review & editing, funding acquisition.

Conflicts of interest

The authors declare that no conflicts of interest.

Appendix A. Supporting information

Supporting information to this article can be found online at https://doi.org/10.1016/j.apsb.2025.11.041.

References

1. Fang C, Fernie AR, Luo J. Exploring the diversity of plant metabolism. *Trends Plant Sci* 2019;**24**:83−98.
2. Rai A, Saito K, Yamazaki M. Integrated omics analysis of specialized metabolism in medicinal plants. *Plant J* 2017;**90**:764−87.
3. Huang L, Guo L, Zhang X, Yu L, Sun J. Species of Chinese materia medica resources based on the fourth national survey of Chinese materia medica resources. *STCM* 2024;**2**:183−6.
4. Huang L. Science of traditional Chinese medicine: an international exchange platform for traditional Chinese medicine. *STCM* 2023;**1**:2.
5. Protection and sustainable utilization of traditional medicinal biogenetic resources. *STCM* 2024;**2**:1−4.
6. Li M, Li Q, Zhang C, Zhang N, Cui Z, Huang L, et al. An ethnopharmacological investigation of medicinal *Salvia* plants (Lamiaceae) in China. *Acta Pharm Sin B* 2013;**3**:273−80.
7. Jia E, Li H, He F, Xu X, Wei J, Shao G, et al. Metabolic engineering of artificially modified transcription factor SmMYB36−VP16 for high-level production of tanshinones and phenolic acids. *Metab Eng* 2024;**86**:29−40.
8. Cheng Y, Luo L, Tang H, Wang J, Ren L, Cui G, et al. Engineering the microenvironment of P450s to enhance the production of

diterpenoids in *Saccharomyces cerevisiae*. *Acta Pharm Sin B* 2024;**14**: 4608−18.
9. Hou Y, Zhong B, Zhao L, Wang H, Zhu Y, Wang X, et al. A small molecule cryptotanshinone induces non-enzymatic NQO1-dependent necrosis in cancer cells through the JNK1/2/Iron/PARP/calcium pathway. *Acta Pharm Sin B* 2025;**15**:991−1006.
10. Ma Y, Yuan L, Wu B, Li X, Chen S, Lu S. Genome-wide identification and characterization of novel genes involved in terpenoid biosynthesis in *Salvia miltiorrhiza*. *J Exp Bot* 2012;**63**:2809−23.
11. Guo J, Zhou YJJ, Hillwigc ML, Shen Y, Yang L, Wang YJ, et al. CYP76AH1 catalyzes turnover of miltiradiene in tanshinones biosynthesis and enables heterologous production of ferruginol in yeasts. *Proc Natl Acad Sci U S A* 2013;**110**:12108−13.
12. Song JJ, Fang X, Li CY, Jiang Y, Li JX, Wu S, et al. A 2-oxoglutarate-dependent dioxygenase converts dihydrofuran to furan in *Salvia* diterpenoids. *Plant Physiol* 2022;**188**:1496−506.
13. Guo J, Ma XH, Cai Y, Ma Y, Zhan ZL, Zhou YJ, et al. Cytochrome P450 promiscuity leads to a bifurcating biosynthetic pathway for tanshinones. *New Phytol* 2016;**210**:525−34.
14. Ma Y, Cui G, Chen T, Ma X, Wang R, Jin B, et al. Expansion within the CYP71D subfamily drives the heterocyclization of tanshinones synthesis in *Salvia miltiorrhiza*. *Nat Commun* 2021;**12**:685.
15. Li Q, Duncan S, Li Y, Huang S, Luo M. Decoding plant specialized metabolism: new mechanistic insights. *Trends Plant Sci* 2024;**29**:535−45.
16. Gantet P, Memelink J. Transcription factors: tools to engineer the production of pharmacologically active plant metabolites. *Trends Pharmacol Sci* 2002;**23**:563−9.
17. Xing B, Sun J, Yu H, Zhang X, Fan K, Liang Z. SmWD40-2 functions as a positive regulator of both tanshinones and phenolic acids biosynthesis in *Salvia miltiorrhiza* Bunge hairy roots. *Ind Crop Prod* 2023;**193**:116219.
18. Li L, Wang DH, Zhou L, Yu XD, Yan XY, Zhang Q, et al. JA-responsive transcription factor SmMYB97 promotes phenolic acid and tanshinone accumulation in *Salvia miltiorrhiza*. *J Agric Food Chem* 2020;**68**:14850−62.
19. Cao R, Lv B, Shao S, Zhao Y, Yang M, Zuo A, et al. The SmMYC2−SmMYB36 complex is involved in methyl jasmonate-mediated tanshinones biosynthesis in *Salvia miltiorrhiza*. *Plant J* 2024; **119**:746−61.
20. Li Q, Fang X, Zhao Y, Cao R, Dong J, Ma P. The SmMYB36−SmERF6/SmERF115 module regulates the biosynthesis of tanshinones and phenolic acids in *Salvia miltiorrhiza* hairy roots. *Hortic Res* 2023;**10**:uhac238.
21. Xing BC, Yang DF, Yu HZ, Zhang BX, Yan KJ, Zhang XM, et al. Overexpression of *SmbHLH10* enhances tanshinones biosynthesis in *Salvia miltiorrhiza* hairy roots. *Plant Sci* 2018;**276**:229−38.
22. Shah SH, Islam S, Mohammad F, Siddiqui MH. Gibberellic acid: a versatile regulator of plant growth, development and stress responses. *J Plant Growth Regul* 2023;**42**:7352−73.
23. Itoh H, Sasaki A, Ueguchi-Tanaka M, Ishiyama K, Kobayashi M, Hasegawa Y, et al. Dissection of the phosphorylation of rice DELLA protein, SLENDER RICE1. *Plant Cell Physiol* 2005;**46**: 1392−9.
24. Lawit SJ, Wych HM, Xu D, Kundu S, Tomes DT. Maize DELLA proteins dwarf plant8 and dwarf plant9 as modulators of plant development. *Plant Cell Physiol* 2010;**51**:1854−68.
25. Li Y, Pang Q, Li B, Fu Y, Guo M, Zhang C, et al. Characteristics of CXE family of *Salvia miltiorrhiza* and identification of interactions between SmGID1s and SmDELLAs. *Plant Physiol Biochem* 2024; **206**:108140.
26. Claeys H, De Bodt S, Inzé D. Gibberellins and DELLAs: central nodes in growth regulatory networks. *Trends Plant Sci* 2014;**19**:231−9.
27. Briones-Moreno A, Hernández-García J, Vargas-Chávez C, Blanco-Touriñán N, Phokas A, Úrbez C, et al. DELLA functions evolved by rewiring of associated transcriptional networks. *Nat Plants* 2023;**9**: 535−43.
28. Li Z, Ahammed GJ. Hormonal regulation of anthocyanin biosynthesis for improved stress tolerance in plants. *Plant Physiol Biochem* 2023; **201**:107835.
29. Li W, Liu C, Liu J, Bai Z, Liang Z. Transcriptomic analysis reveals the GRAS family genes respond to gibberellin in *Salvia miltiorrhiza* hairy roots. *BMC Genom* 2020;**21**:727.
30. Yu H, Li D, Yang D, Xue Z, Li J, Xing B, et al. SmKFB5 protein regulates phenolic acid biosynthesis by controlling the degradation of phenylalanine ammonia-lyase in *Salvia miltiorrhiza*. *J Exp Bot* 2021; **72**:4915−29.
31. Livak KJ, Schmittgen TD. Analysis of relative gene expression data using real-time quantitative PCR and the $2^{-\Delta\Delta CT}$ method. *Methods* 2001;**25**:402−8.
32. Li D, Zheng C, Zhou J, Chen B, Xu R, Yuan W, et al. pGP-B2E, a recombinant compatible TA/TB-ligation vector for rapid and inexpensive gene cloning. *Mol Biotechnol* 2020;**62**:56−66.
33. Yu HZ, Guo WL, Yang DF, Hou ZN, Liang ZS. Transcriptional profiles of SmWRKY family genes and their putative roles in the biosynthesis of tanshinone and phenolic acids in *Salvia miltiorrhiza*. *Int J Mol Sci* 2018;**19**:1593.
34. Abramson J, Adler J, Dunger J, Evans R, Green T, Pritzel A, et al. Accurate structure prediction of biomolecular interactions with AlphaFold 3. *Nature* 2024;**630**:493−500.
35. Xie X, Ma X, Zhu Q, Zeng D, Li G, Liu YG. CRISPR-GE: a convenient software toolkit for CRISPR-based genome editing. *Mol Plant* 2017;**10**:1246−9.
36. Wang ZP, Xing HL, Dong L, Zhang HY, Han CY, Wang XC, et al. Egg cell-specific promoter-controlled CRISPR/Cas9 efficiently generates homozygous mutants for multiple target genes in Arabidopsis in a single generation. *Genome Biol* 2015;**16**:144.
37. Wang F, Zhu D, Huang X, Li S, Gong Y, Yao Q, et al. Biochemical insights on degradation of Arabidopsis DELLA proteins gained from a cell-free assay system. *Plant Cell* 2009;**21**:2378−90.
38. Gao F, Dubos C. The arabidopsis bHLH transcription factor family. *Trends Plant Sci* 2024;**29**:668−80.
39. Qi T, Huang H, Wu D, Yan J, Qi Y, Song S, et al. Arabidopsis DELLA and JAZ proteins bind the WD-Repeat/bHLH/MYB complex to modulate Gibberellin and Jasmonate signaling synergy. *Plant Cell* 2014;**26**:1118−33.
40. Liu F, Xi M, Liu T, Wu X, Ju L, Wang D. The central role of transcription factors in bridging biotic and abiotic stress responses for plants' resilience. *New Crops* 2024;**1**:100005.
41. Sun Y, Fernie AR. Plant secondary metabolism in a fluctuating world: climate change perspectives. *Trends Plant Sci* 2024;**29**:560−71.
42. Du Q, Li C, Li D, Lu S. Genome-wide analysis, molecular cloning and expression profiling reveal tissue-specifically expressed, feedback-regulated, stress-responsive and alternatively spliced novel genes involved in gibberellin metabolism in *Salvia miltiorrhiza*. *BMC Genom* 2015;**16**:1087.
43. Timp W, Timp G. Beyond mass spectrometry, the next step in proteomics. *Sci Adv* 2020;**6**:eaax8978.
44. Li L, Hao XL, Liu H, Wang W, Fu XQ, Ma YN, et al. Jasmonic acid-responsive AabHLH1 positively regulates artemisinin biosynthesis in *Artemisia annua*. *Biotechnol Appl Biochem* 2019;**66**:369−75.
45. Ye JB, Yang K, Li YT, Xu F, Cheng SY, Zhang WW, et al. Genome-wide transcriptome analysis reveals the regulatory network governing terpene trilactones biosynthesis in *Ginkgo biloba*. *Tree Physiol* 2022; **42**:2068−85.
46. Du T, Niu J, Su J, Li S, Guo X, Li L, et al. SmbHLH37 functions antagonistically with SmMYC2 in regulating jasmonate-mediated biosynthesis of phenolic acids in *Salvia miltiorrhiza*. *Front Plant Sci* 2018;**9**:1720.
47. Xue XS, Li L, Wang DH, Zhou W, Wang ZZ, Cao XY. SmJAZ1/8 inhibits the stimulation of SmbHLH59, which limits the accumulation of salvianolic acids and tanshinones in *Salvia miltiorrhiza*. *Int J Biol Macromol* 2025;**285**:138348.

48. Wang X, Chai X, Gao B, Deng C, Günther CS, Wu T, et al. Multi-omics analysis reveals the mechanism of bHLH130 responding to low-nitrogen stress of apple rootstock. *Plant Physiol* 2023;**191**:1305−23.
49. Nützmann HW, Scazzocchio C, Osbourn A. Metabolic gene clusters in eukaryotes. *Annu Rev Genet* 2018;**52**:159−83.
50. Nutzmann HW, Osbourn A. Gene clustering in plant specialized metabolism. *Curr Opin Biotechnol* 2014;**26**:91−9.
51. Lanier ER, Andersen TB, Hamberger B. Plant terpene specialized metabolism: complex networks or simple linear pathways? *Plant J* 2023;**114**:1178−201.
52. Deng CP, Hao XL, Shi M, Fu R, Wang Y, Zhang Y, et al. Tanshinone production could be increased by the expression of *SmWRKY2* in *Salvia miltiorrhiza* hairy roots. *Plant Sci* 2019;**284**:1−8.
53. Zheng H, Jing L, Jiang X, Pu C, Zhao S, Yang J, et al. The ERF-VII transcription factor SmERF73 coordinately regulates tanshinone biosynthesis in response to stress elicitors in *Salvia miltiorrhiza. New Phytol* 2021;**231**:1940−55.
54. Xing BC, Qiu L, Wang ZX, Wang FY, Yu HZ, Li W, et al. A novel synergistic regulatory mechanism involving the MYB39-MYB111-bHLH51-TTG1 module in the phenolic and diterpenoid biosynthetic pathways of *Salvia miltiorrhiza*. *Plant Biotechnol J* 2025;**23**:4367−80.
55. Xu Y, Du J, Hao R, Ma S, Ma Y, Zhou G, et al. Gibberellin signaling regulates pectin biosynthesis in *Arabidopsis*. *Nat Commun* 2025;**16**: 4065.
56. Qu SS, Li MM, Wang G, Zhu SJ. Application of ABA and GA_3 alleviated browning of litchi (*Litchi chinensis* Sonn.) *via* different strategies. *Postharvest Biol Technol* 2021;**181**:111672.
57. Tao H, Gao F, Linying L, He Y, Zhang X, Wang M, et al. WRKY33 negatively regulates anthocyanin biosynthesis and cooperates with PHR1 to mediate acclimation to phosphate starvation. *Plant Commun* 2024;**5**:100821.
58. Li Y, Chen J, Zhi J, Huang D, Zhang Y, Zhang L, et al. The ABC transporter SmABCG1 mediates tanshinones export from the peridermic cells of *Salvia miltiorrhiza* root. *J Integr Plant Biol* 2024;**67**:135−49.
59. Xu H, Liu Q, Yao T, Fu X. Shedding light on integrative GA signaling. *Curr Opin Plant Biol* 2014;**21**:89−95.
60. He Z, Zhang P, Jia H, Zhang S, Nishawy E, Sun X, et al. Regulatory mechanisms and breeding strategies for crop drought resistance. *New Crops* 2024;**1**:100029.
61. Hong GJ, Xue XY, Mao YB, Wang LJ, Chen XY. Arabidopsis MYC2 interacts with DELLA proteins in regulating sesquiterpene synthase gene expression. *Plant Cell* 2012;**24**:2635−48.